frontiers in Marine Science

ORIGINAL RESEARCH
published: 20 December 2021
doi: 10.3389/fmars.2021.737886

Interspecific Analysis of Sea Urchin Adhesive Composition Emphasizes Variability of Glycans Conjugated With Putative Adhesive Proteins

*Lisa Gaspar[1], Patrick Flammang[2], Ricardo José[3,4], Ricardo Luis[3,4], Patrício Ramalhosa[4,5], João Monteiro[5], Natacha Nogueira[3,4], João Canning-Clode[5,6] and Romana Santos[1,7]**

[1] Centro de Ciências do Mar e do Ambiente (MARE), Faculdade de Ciências, Universidade de Lisboa, Lisbon, Portugal, [2] Biology of Marine Organisms and Biomimetics Unit, Research Institute for Biosciences, University of Mons, Mons, Belgium, [3] Centro de Maricultura da Calheta (CMC), Direção Regional do Mar, Calheta, Portugal, [4] Observatório Oceânico da Madeira (OOM), Agência Regional para o Desenvolvimento da Investigação, Tecnologia e Inovação (ARDITI), Funchal, Portugal, [5] Centro de Ciências do Mar e do Ambiente (MARE), Agência Regional para o Desenvolvimento da Investigação, Tecnologia e Inovação (ARDITI), Funchal, Portugal, [6] Smithsonian Environmental Research Center, Edgewater, MD, United States, [7] Departamento de Biologia Animal, Faculdade de Ciências, Universidade de Lisboa, Lisbon, Portugal

OPEN ACCESS

Edited by:
Maria Bebianno,
University of Algarve, Portugal

Reviewed by:
Nick Aldred,
University of Essex, United Kingdom
Shiguo Li,
Research Center for Eco-Environmental Sciences, Chinese Academy of Sciences (CAS), China
Lisheng He,
Institute of Deep-Sea Science and Engineering, Chinese Academy of Sciences (CAS), China

***Correspondence:**
Romana Santos
rlasantos@fc.ul.pt

Specialty section:
This article was submitted to Marine Ecosystem Ecology, a section of the journal Frontiers in Marine Science

Received: 07 July 2021
Accepted: 29 November 2021
Published: 20 December 2021

Citation:
Gaspar L, Flammang P, José R, Luis R, Ramalhosa P, Monteiro J, Nogueira N, Canning-Clode J and Santos R (2021) Interspecific Analysis of Sea Urchin Adhesive Composition Emphasizes Variability of Glycans Conjugated With Putative Adhesive Proteins. Front. Mar. Sci. 8:737886. doi: 10.3389/fmars.2021.737886

Sea urchins possess specialized adhesive organs, tube feet. Although initially believed to function as suckers, it is currently accepted that they rely on adhesive and de-adhesive secretions to attach and detach repeatedly from the substrate. Given the biotechnological potential of their strong reversible adhesive, sea urchins are under investigation to identify the protein and glycan molecules responsible for its surface coupling, cohesion and polymerization properties. However, this characterization has only focused on a single species, *Paracentrotus lividus*. To provide a broader insight into sea urchins adhesion, a comparative study was performed using four species belonging to different taxa and habitats: *Diadema africanum*, *Arbacia lixula*, *Paracentrotus lividus* and *Sphaerechinus granularis*. Their tube feet external morphology and histology was studied, together with the ultrastructure of their adhesive secretory granules. In addition, one antibody and five lectins were used on tube foot histological sections and extracts, and on adhesive footprints to detect the presence of adhesion-related (glyco)proteins like those present in *P. lividus* in other species. Results confirmed that the antibody raised against *P. lividus* Nectin labels the adhesive organs and footprints in all species. This result was further confirmed by a bioinformatic analysis of Nectin-like sequences in ten additional species, increasing the comparison to seven families and three orders. The five tested lectins (GSL II, WGA, STL, LEL, and SBA) demonstrated that there is high interspecific variability of the glycans involved in sea urchin adhesion. However, there seems to be more conservation among taxonomically closer species, like *P. lividus* and *S. granularis*. In these species, lectin histochemistry and lectin blots indicated the presence of high molecular weight putative adhesive glycoproteins bearing N-acetylglucosamine residues in the form of chitobiose in the adhesive epidermis

and footprints. Our results emphasize a high selective pressure for conservation of functional domains in large putative cohesive proteins and highlight the importance of glycosylation in sea urchin adhesion with indications of taxonomy-related conservation of the conjugated glycans.

Keywords: sea urchins, Echinoidea, tube feet, footprint, temporary adhesion, proteins, glycans

INTRODUCTION

Echinoderms produce strong reversible adhesives secreted by unique hydraulic adhesive organs called tube feet. The comprehension of this temporary adhesion has motivated several morphological, biomechanical, and biochemical studies in the last decades (Davey et al., 2021).

Adoral tube feet, in particular, are well adapted for locomotion and attachment. They possess a mobile extensible stem, topped by an adhesive viscoelastic disc (Santos and Flammang, 2005; Santos et al., 2005). In sea stars (Asteroidea), three tube foot morphotypes have been described (simple disc-ending, reinforced disc-ending and knob-ending) based on the histological structure of their disc (Santos et al., 2005). In regular sea urchins (Echinoidea), all tube feet are reinforced-disc ending, but they have been subcategorized based on the size of their disc and thickness of their stem connective tissue and retractor muscle (type 4 > 3 > 2 > 1) (Smith, 1978). These morphological differences were pointed as essential for tube feet attachment strength and consequently, for species distribution (Smith, 1978).

However, more recent biomechanical studies with three Mediterranean sea urchin species, *Arbacia lixula* (Linnaeus, 1758), *Paracentrotus lividus* (Lamark, 1816) and *Sphaerechinus granularis* (Lamark, 1816), and four Indian Ocean species, *Colobocentrotus atratus* (Linnaeus, 1758), *Echinometra mathaei* (Blainville, 1825), *Heterocentrotus trigonarius* (Lamarck, 1816) and *Stomopneustes variolaris* (Lamarck, 1816), belonging to three orders and five families of the Class Echinoidea, found no correlation between interspecific variations in disc tenacity (force per unit area) and the disc adhesive area (Santos and Flammang, 2006, 2008). In addition, when a tensile force is exerted on a tube foot stem, it is the connective tissue that bears the load, and not the muscle (Santos and Flammang, 2005, 2008).

Furthermore, in the three Mediterranean species significant variations in the ultrastructure of the adhesive secretory granules were reported, suggesting that there might be molecular differences in the composition of their adhesive secretions (Santos and Flammang, 2006). To test this hypothesis an antibody raised against *S. granularis* adhesive material was tested for cross-reactivity on tube foot histological sections from the above-mentioned species, plus *Tripneustes gratilla* (Linnaeus, 1776) (Santos and Flammang, 2012). This approach was used to bypass the need for complete characterization of echinoid adhesives and because it successfully evidenced the compositional similarity of sea star adhesive footprints at the class level (Santos et al., 2005). Surprisingly, in sea urchins no cross-reactivity was observed in any species tested, not even in *T. gratilla* that belongs to the same family as *S. granularis* (Santos and Flammang, 2012).

After these findings, several biochemical studies attempted to fully characterize the adhesive material but focused exclusively on *Paracentrotus lividus*. The analysis of adhesive footprints showed that they consisted of a honeycomb-like meshwork of aggregated globular nanostructures (Viana and Santos, 2018) composed of proteins, neutral sugars, lipids and inorganic residues (Santos et al., 2009). The adhesive material proteome revealed a prevalence of five protein groups (actins, tubulins, myosins, ribosomal proteins and histones) and only one cell-adhesion protein, *P. lividus* Nectin (Lebesgue et al., 2016). A recent re-analysis of this proteome using a tube foot specific transcriptome, combined with a quantitative proteome analysis of the adhesive disc versus the non-adhesive stem, and a validation of gene expression using *in situ* hybridization (ISH), drastically increased the mapped proteins and highlighted sixteen transcripts potentially involved in bioadhesion (Pjeta et al., 2020). Of these, six transcripts (Nectin, alpha-tectorin, uncharacterized protein, Myeloperoxidase, neurogenic locus notch homolog protein and alpha-macroglobulin) presented a ISH expression pattern consistent with the location of the adhesive secretory cell bodies, and simultaneously possessed an ortholog adhesion-related transcript in the sea star *Asterias rubens* (Linnaeus, 1758) (Lengerer et al., 2019; Pjeta et al., 2020).

P. lividus-Nectin is a 210-kDa homodimer glycoprotein consisting of two polypeptides with an equal mass of 105 kDa each, joining covalently by S–S bridges (Zito et al., 1998). It contains 6 tandemly repeated discoidin-like (or F5/8 type C) domains predicted to bind molecules bearing galactose and N-acetylglucosamine carbohydrate moieties (Costa et al., 2010), and a LDT motif predicted to be the binding site to an α4/β7 integrin receptor (Zito et al., 2010). It was first discovered in the extracellular matrix (ECM) of *P. lividus* embryos. It is also present in the unfertilized egg cytoplasm, stored in granules, and is released into the ECM surrounding the embryo after fertilization. In later developmental stages, it polarizes on the apical surface of ectodermal and endodermal cells. Thus, *P. lividus*-Nectin is involved in cell adhesion processes as an integrin ligand and its contact to ectodermal cells is essential for correct larval skeletogenesis (Zito et al., 2000, 2010; Costa et al., 2010).

Nectin was first related to adult *P. lividus* adhesion when it was identified both in tube feet and adhesive footprints using antibodies raised against embryonic Nectin (Lebesgue et al., 2016). Although present in both the tube foot disc and stem, it was shown to be highly overexpressed at the mRNA and protein level in the adhesive discs, being regulated by the degree of hydrodynamism to which the sea urchin is exposed (Lebesgue et al., 2016; Toubarro et al., 2016). So far, in adult *P. lividus* tube feet, three Nectin variants, the embryonic Nectin (variant 1 – Uniprot Q70JA0) plus two others (variant 2 – Uniprot

A0A182BBB6; variant 3 – tube foot transcriptome), differing in only a few amino acid substitutions, have been reported (Lebesgue et al., 2016; Toubarro et al., 2016; Pjeta et al., 2020). In addition, several Nectin isoforms have been observed in 2DE gels, presenting different degrees of phosphorylation and glycosylation (Santos et al., 2013).

The remaining five *P. lividus* transcripts potentially involved in bioadhesion (Pjeta et al., 2020) possess domains that are recurrent in other marine adhesive and cohesive proteins (Davey et al., 2021) but require further investigation. *P. lividus* alpha-tectorin shares domains present in adhesive proteins from sea stars (Sfp1; Hennebert et al., 2014), flatworms (Mlig-ap1 and −2, Mile-ap1 and Mile-ap2a/b; Pjeta et al., 2019; Wunderer et al., 2019), cnidarians (Rodrigues et al., 2016) and a terrestrial slug (Smith et al., 2017). The identification of Myeloperoxidase in *P. lividus* (Lebesgue et al., 2016; Pjeta et al., 2020) agrees with reports of peroxidase-like proteins being present in the adhesive secretions of sea star (Hennebert et al., 2015), cnidarians (Rodrigues et al., 2016), caddisfly larvae (Wang et al., 2014), and adult barnacles (So et al., 2017). Peroxidases are believed to act as catalyzers of protein crosslinking within the adhesive, thus, contributing to its high cohesive strength (Pjeta et al., 2020). *P. lividus* neurogenic locus notch homolog protein contains trypsin inhibitor-like cysteine-rich domains, also present in sea star Sfp1 (Hennebert et al., 2014), that can form disulfide bonds and possibly contribute to echinoderm adhesive insolubility attributed to the presence of proteins with significant amounts of cysteines (Santos et al., 2009; Pjeta et al., 2020). Finally, *P. lividus* alpha-macroglobulin share common domains with several proteins present in the adhesive secretions of sea stars (Hennebert et al., 2015; Lengerer et al., 2019), limpets (Kang et al., 2020), tunicates (Li et al., 2019) and barnacle larvae (Dreanno et al., 2006; Ferrier et al., 2016).

The glycosidic fraction of the adhesive material has also been studied in *P. lividus*, demonstrating the involvement of high molecular weight glycoproteins containing N-acetyl glucosamine residues. Five lectins (GSL II, WGA, STL, LEL, and SBA) out of 22 specifically labeled the disc adhesive epidermis and the adhesive footprints and detected several disc specific glycoproteins (Simão et al., 2020). Of these, LEL, that recognizes N-acetyl glucosamine in a chitobiose arrangement [GlcNAc β(1,4)GlcNAc], specifically labeled the adhesive secretory granules within the characteristic sea urchin 'apical tuft' secretory cells and produced an intense labeling of the footprint, indicating that a glycoprotein containing chitobiose is most likely a main component of *P. lividus* adhesive secretion (Simão et al., 2020). This agrees with growing evidence showing the importance of glycoproteins in marine adhesives, from permanent (mussels, barnacles, algal spores) to non-permanent ones, such as transitory (limpets, marsh periwinkle) or temporary (sea stars, flatworms, ascidian larvae) adhesives (Dreanno et al., 2006; Hennebert et al., 2011; Ferrier et al., 2016; Pjeta et al., 2019; Wunderer et al., 2019; Zeng et al., 2019; Kang et al., 2020).

In this context, the present study aims at unraveling the evolutionary history of adhesion among echinoids by comparing, in terms of the adhesive composition, *P. lividus* with three sympatric species occurring in Madeira Island (NE Atlantic) that belong to different taxa and bear tube feet with different morphologies. *P. lividus* Nectin sequence was used to identify homologous sequences in publicly available echinoid proteomes and transcriptomes. In addition, an immunohistochemical analysis using antibodies against Nectin was performed on tube foot histological sections and adhesive footprints. These antibodies were also used on western blots to detect these proteins in tube foot disc and stem extracts. The conservation of the glycosidic fraction was also approached using the five lectins that detected adhesion-specific glycoproteins in *P. lividus*, by looking for cross-reactivity on histological sections and in blotting assays with the remaining species.

MATERIALS AND METHODS

Nectin Sequences Collection and Alignments

To date, three Nectin protein sequences have been found in the tube feet of individuals of *P. lividus*: Q70JA0 (Costa et al., 2010), A0A182BBB6 (Toubarro et al., 2016) and TR60905_c1_g1_i1_5 (Pjeta et al., 2020). They were used to retrieve homologous sea urchin sequences by performing BLAST (Basic Local Alignment Search Tool) searches (using the default settings) in four publicly available databases: UniprotKB,[1] Transcriptome Shotgun Assembly Sequence Database,[2] EchinoBase,[3] and HpBase.[4] A multiple alignment was performed with COBALT,[5] and a tree from given distances between sequences (maximum sequence distance of 0.85) was produced using the algorithm Fast Minimum Evolution (Desper and Gascuel, 2004).

Sample Collection and Maintenance

Adult sea urchins of the species *Arbacia lixula* (Linnaeus, 1758) and *Paracentrotus lividus* (Lamark, 1816) were collected intertidally at Madeira Island, whereas individuals of *Sphaerechinus granularis* (Lamark, 1816) and *Diadema africanum* Rodríguez et al. 2013 were collected by scuba diving. All sea urchins were kept in open flow aquaria (50 L) or individual containers (10 L) with aeration at room temperature between 20 and 22°C and 35 PSU, respectively at the mesocosm system in the laboratory facilities of the Madeira research unit of MARE, located at Quinta do Lorde Marina or at the laboratory facilities of Calheta Mariculture Center.

Sea urchins were placed upside down in containers filled with seawater and their adoral tube feet sectioned at the base of the stem close to the test. Tube feet were then either stored in 70% ethanol, preserved in RNAlater at 4°C, or fixed by immersion in non-acetic Bouin's fluid or 3% glutaraldehyde in cacodylate buffer (0.1 M. pH 7.8, with 1.55% NaCl).

To collect adhesive footprints, clean microscope glass slides were presented to adoral tube feet to induce attachment. After

[1]https://www.uniprot.org

[2]https://www.ncbi.nlm.nih.gov/genbank/tsa/

[3]http://legacy.echinobase.org/Echinobase/About

[4]http://cell-innovation.nig.ac.jp/Hpul/

[5]https://www.ncbi.nlm.nih.gov/tools/cobalt/re_cobalt.cgi

tube foot detachment, glass slides were abundantly washed with distilled water, allowed to dry, and stored at 4°C until usage.

Scanning and Transmission Electron Microscopy

For SEM, samples were prepared as described by Santos and Flammang (2006). Bouin's fluid-fixed tube feet were dehydrated in graded ethanol, dried by the critical point method, mounted on aluminum stubs, coated with gold in a sputter coater and observed with a JEOL JSM-7200F field emission scanning electron microscope.

For TEM, glutaraldehyde-fixed tube feet were rinsed in cacodylate buffer (0.2 M. pH7.8, with 1.84% NaCl) and then post-fixed in 1% osmium tetroxide in cacodylate buffer (0.1 M. pH7.8, with 2.3% NaCl). After rinsing in cacodylate buffer, they

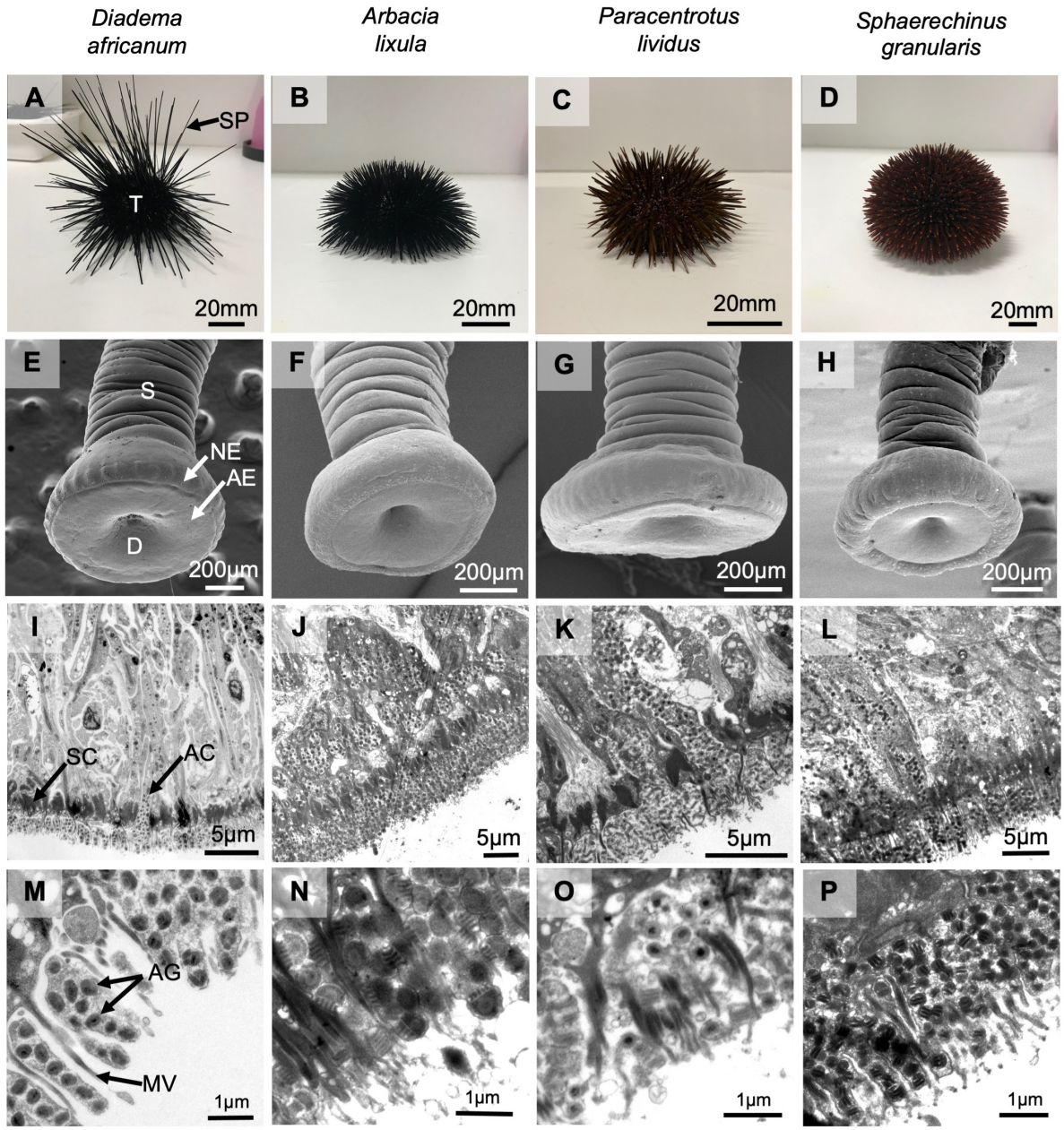

FIGURE 1 | Echinoids used in this study: *Diadema africanum* **(A,E,I,M)**, *Arbacia lixula* **(B,F,J,N)**, *Paracentrotus lividus* **(C,G,K,O)** and *Sphaerechinus granularis* **(D,H,L,P)**. Lateral view of whole sea urchins with spines **(A–D)**. External morphology (SEM) of non-attached adoral tube feet **(E–H)**. General view of the ultrastructure (TEM) of longitudinal sections through the disc of adoral tube feet **(I–L)** and a more detailed view of secretory cells containing adhesive granules **(M–P)**. AC, adhesive secretory cell; AE, adhesive epidermis; AG, adhesive granule; D, disc; MV, microvillar-like cell projection; NE, non-adhesive epidermis; S, stem; SC, support cell; SP, spine; T, test.

were de-hydrated in graded ethanol and embedded in Spurr resin. Ultrathin sections (80 nm) were cut with a Leica Ultracut UCT ultramicrotome equipped with a diamond knife. They were contrasted with uranyl acetate and lead citrate and observed with a Zeiss LEO 906E transmission electron microscope.

Histological Staining and Histochemistry

Bouin's fluid-fixed tube feet were rinsed in 70% ethanol, then decalcified with a 1:1 solution of 2% ascorbic acid and 0.3 M NaCl for 24 h at RT with constant rotation. Next, they were dehydrated in graded ethanol, embedded in paraffin wax and cut longitudinally into 7 μm thick sections with a microtome (Leica RM 2155). After dewaxing and rehydration, two histological stains (Masson's trichrome and Alcian Blue pH 2.5) and two histochemical techniques (immuno- and lectin-histochemistry) were performed on tube foot sections and footprints. Due to strong tube foot pigmentation, the sections from *D. africanum* and *A. lixula* had to be incubated in 10% (v/v) hydrogen peroxide in phosphate-buffered saline (PBS) for 30 min at 65°C before experiments.

For immunohistochemistry, the protocol of Santos and Flammang (2012) was followed with some adaptations. Briefly, tube foot sections were incubated in 50 mM NH_4Cl for 15 min to block free aldehyde groups from the fixative, followed by permeabilization in PBS with 0.25% Triton-X-100 for 1 h, and by preincubation for 30 min with 10% normal donkey serum. Sections were incubated overnight at 4°C with polyclonal anti-*Paracentrotus lividus* Nectin polyclonal antibody (kindly provided by Dr. Francesca Zito) diluted 1:400 in PBS-T-BSA [PBS, 1% (v/v) Tween-20, 1% (w/v) BSA]. Alexa Fluor 568-conjugated donkey-anti-rabbit IgG (Invitrogen) were diluted 1:1000 in PBS-T-BSA and applied for 1 h at room temperature. Then, sections were incubated for 5 min with TrueVIEW (Vector), followed by 1 min with DAPI (4',6-diamino-2-phenylindole, Invitrogen), mounted in Vibrance Mounting Medium (Vector) and analyzed with an Olympus BX60 epifluorescence microscope. Footprints were first rehydrated in ultrapure water and the procedure described above applied from the incubation with 10% normal donkey serum onward.

Lectin-histochemistry was performed according to Simão et al. (2020). Footprints and sections were blocked with TBS-T-BSA [10 mM Tris-HCl, 150 mM NaCl (w/v), pH 8, 0,05% (v/v) Tween-20, 3% (w/v) BSA] for 2 h at room temperature. Afterward, the five biotinylated lectins (GSL II, WGA, STL, LEL and SBA, see **Supplementary Table 1**), diluted in TBS-T-BSA supplemented with ions (1 mM $CaCl_2$, 1 mM $MnCl_2$), were applied to the samples and incubated for 2 h at room temperature. This was followed by incubation for 1 h at RT with Alexa Fluor 488-conjugated streptavidin (Invitrogen, United States) in TBS-T-BSA (see **Supplementary Table 1**). Incubation with DAPI, mounting and visualization were performed as described above.

Control reactions were performed replacing antibodies and lectins with PBS-T-BSA or TBS-T-BSA, respectively.

Since footprints fluorescence is dependent on the amount of adhesive material deposited by each echinoid, the obtained fluorescence microscopy images were used to calculate the footprint total corrected fluorescence (FTCF) using the software Fiji ImageJ. This calculation allows subtracting the background from the fluorescence observed in the footprint area, providing an actual fluorescence value per unit area [FTCF = (Area of selected footprint × Mean fluorescence of footprint) – (Area of selected footprint × Mean fluorescence of background)]. The statistical significance of interspecific differences was determined by 1-way ANOVA, with a p-value <0.05 indicating a statistically significant difference. Normality was checked using Shapiro Wilks, as well as homoscedasticity using the Levene's test.

Protein Extraction, Separation, and Blotting

These procedures were performed as reported by Simão et al. (2020). Succinctly, proteins were extracted from RNAlater-preserved disc and stem samples by combining chemical lysis, using RIPA buffer (150 mM NaCl, 1.0% Triton X-100, 0.5% sodium deoxycholate, 0.1% SDS, 50 mM Tris, pH 8.0) supplemented with a protease and phosphatase inhibitor cocktail at a dilution of 1:10,000 (Sigma), and mechanical lysis using in a ball mill (Retsch MM400, Germany) for 10 min. Afterward, samples were centrifuged at 14,000 rpm for 10 min at 4°C and the supernatant collected and kept at −20°C until further use. The samples' total protein concentration was determined using the Bradford colorimetric microplate assay (Bio-Rad, United States) and absorbances were obtained at a wavelength of 595 nm. Next, protein separation was performed by SDS-PAGE, followed by protein transfer to a polyvinylidene fluoride (PVDF) membrane. The membrane was blocked overnight TBS-T with 5% skimmed milk (for antibodies) or TBS-T-BSA (for lectins) at 4°C with constant agitation and then incubated for 1 h 30 min with the antibody diluted 1:1000 in TBS-T with 1% skimmed milk or with one of the five biotinylated lectins diluted to a concentration of 1μg/ml in TBS-T-BSA-ions. After rinsing, the membrane was incubated for 1 h with horseradish peroxidase-conjugated anti-rabbit IgG antibody (ThermoFisher) or -streptavidin (Vector Laboratories) diluted 1:5000 in TBS-T-BSA. (Glyco)proteins were visualized using an ECL immunoblot detection system (Amersham GE Healthcare, United Kingdom) and a CCD Imager 680 RGB (Amersham GE Healthcare, United Kingdom).

RESULTS

Echinoids From Different Habitats Show Variable Tube Foot Morphology and Ultrastructure

The four sympatric species under analysis possess tests and spines with very different dimensions. *A. lixula* and *P. lividus*, that are typical of the intertidal, are smaller and have more flattened tests. In contrast, *D. africanum* and *S. granularis*, typical from the subtidal, present larger and rounder tests and, in *D. africanum*, characteristic long spines (**Figures 1A–D**). The external morphology of their tube feet is quite similar,

being composed of discs that are wider than the stems. SEM observations confirmed that all the species presented a disc with two distinct parts, a peripheral area and a central area showing a depression in non-attached tube feet (**Figures 1E–H**), corresponding to the non-adhesive and adhesive epidermis, respectively. Internally, the histological structure of the tube feet of all the species was quite constant, being composed of a myomesothelium surrounding the water-vascular lumen, a connective tissue layer, a nerve plexus and an outer epidermis covered externally by a cuticle (**Figures 2A–D**). However, the degree of development of these tissue layers is not identical in the tube feet of all species. The myomesothelium (both levator and retractor muscle) is thinner in *D. africanum* and *S. granularis*, thicker in *A. lixula*, and intermediate in *P. lividus*. The connective tissue, is less developed in *D. africanum*, moderately developed in *S. granularis* and *P. lividus*, and well developed in *A. lixula*, with visible collagen fibers that maneuver themselves between the skeletal structures, the epidermis, up to the cuticle (**Figures 2A–D**). TEM observations of the disc adhesive epidermis show that all the species possess clusters of four cell types: support cells, sensory cells, adhesive secretory cells, and de-adhesive secretory cells (**Figures 1I–L**). However, a closer look at the ultrastructure of the adhesive granules highlights a considerable variability in terms of size and internal organization. *D. africanum* (**Figure 1M**) and *P. lividus* (**Figure 1O**) have granules with a small electron dense core, surrounded by a large electron lucent rim, while *A. lixula* (**Figure 1N**) and *S. granularis* (**Figure 1P**) have granules with

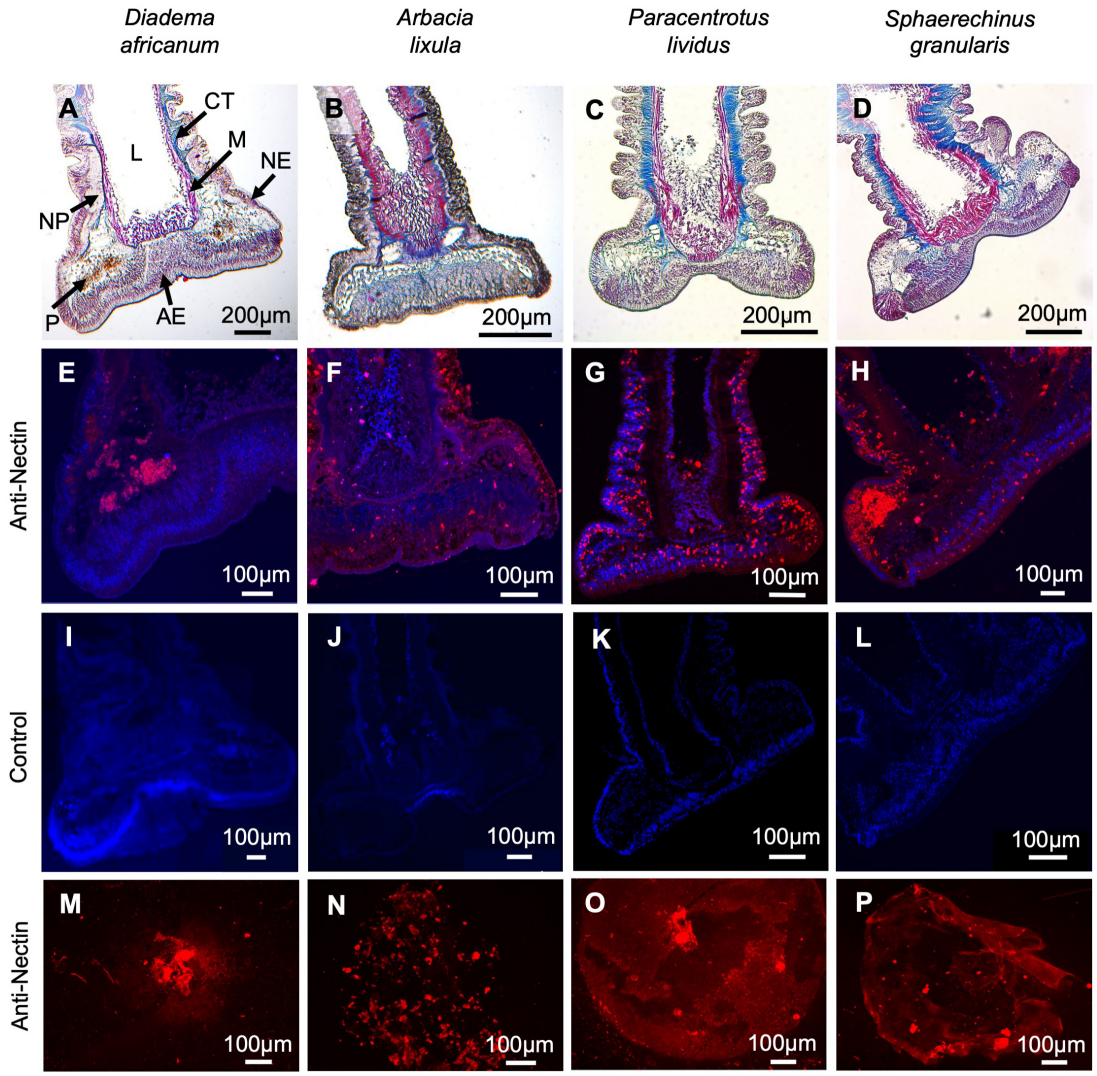

FIGURE 2 | Histological structure and immunohistochemistry of longitudinal section through adoral tube feet and of footprints from *Diadema africanum* **(A,E,I,M)**, *Arbacia lixula* **(B,F,J,N)**, *Paracentrotus lividus* **(C,G,K,O)** and *Sphaerechinus granularis* **(D,H,L,P)**. Staining with Masson's Trichrome **(A–D)**. Labeling (in red) with anti-*P. lividus* Nectin antibody of longitudinal section through adoral tube feet **(E–H)** and of footprints **(I–L)**. Negative controls **(M–P)** in which the primary antibody has been replaced by buffer. AE, adhesive epidermis; CT, connective tissue; L, lumen; M, myomesothelium; NE, non-adhesive epidermis; NP, nerve plexus, P, pigment cells.

a highly organized core with electron-dense parallel plates, surrounded by an electron-lucent material. In terms of size, *D. africanum* and *S. granularis* presented the smallest granules (200–350 and 300–400 nm in diameter, respectively), while *P. lividus* and *A. lixula* possess larger granules (300–500 and 400–700 nm in diameter, respectively).

Occurrence of Nectin in Sea Urchins From Different Echinoid Orders and Families

P. lividus Nectin sequences (UniprotKB, Transcriptome Shotgun Assembly Sequence Database, and protein translated from tube foot mRNA TR60905_c1_g1_i1_5, Pjeta et al., 2020) were used to identify homologous sequences from other echinoids in publicly available datasets. Nectin-like sequences were retrieved for nine other echinoid species belonging to six families and three orders: *Arbacia punctulata*, *Eucidaris tribuloides*, *Evechinus chloroticus*, *Hemicentrotus pulcherrimus*, *Loxechinus albus*, *Lytechinus variegatus*, *Mesocentrotus franciscanus*, *Sphaerechinus granularis and Strongylocentrotus purpuratus*.

The obtained sequence alignment (**Supplementary Figure 1** and **Supplementary Table 2**) and summary tree (**Figure 3**) demonstrates that Nectin-like proteins are present in all the analyzed species, representative of three orders (Cidaroida, Arbacioida, Camarodonta) and six families (Cidaridae, Arbaciidae, Toxopneustidae, Strongylocentrotidae, Echinometridae and Echinidae). Interestingly, the protein sequence grouping in **Figure 3** matches the phylogenetic tree for these echinoids (Koch and Thompson, 2020), revealing that closely related species such as the Echinidae *P. lividus* and *L. albus* (78–80% identity), the Toxopneustidae *S. granularis* and *L. variegatus* (86–89% identity), and the Strongylocentrotidae *M. fransciscanus*, *S. purpuratus* and *H. pulcherimmus* (84–94% identity), have Nectins with higher sequence homology. There is also clustering of the species belonging to the order Camarodonta, which share higher sequence homologies within the order (44–80% identity) than with *A. punctulata* 49–67% identity) or *E. tribuloides* (62–68% identity) that belong respectively to the order Arbacioida and Cidaroida (**Supplementary Table 2**). However, it should be noted that most of these sequences correspond to embryonic Nectins as tube foot transcriptomes are rarely available.

These results were complemented with immunohistochemical and western blot analyses using an antibody produced against *P. lividus* Nectin. Tube foot sections of the four Madeira echinoids probed with anti-*P. lividus* Nectin antibody exhibited small immunoreactive dots along the disc adhesive epidermis but also the stem non-adhesive epidermis in *A. lixula* (**Figures 2F,J**), *P. lividus* (**Figures 2G,K**) and *S. granularis* (**Figures 2H,L**).

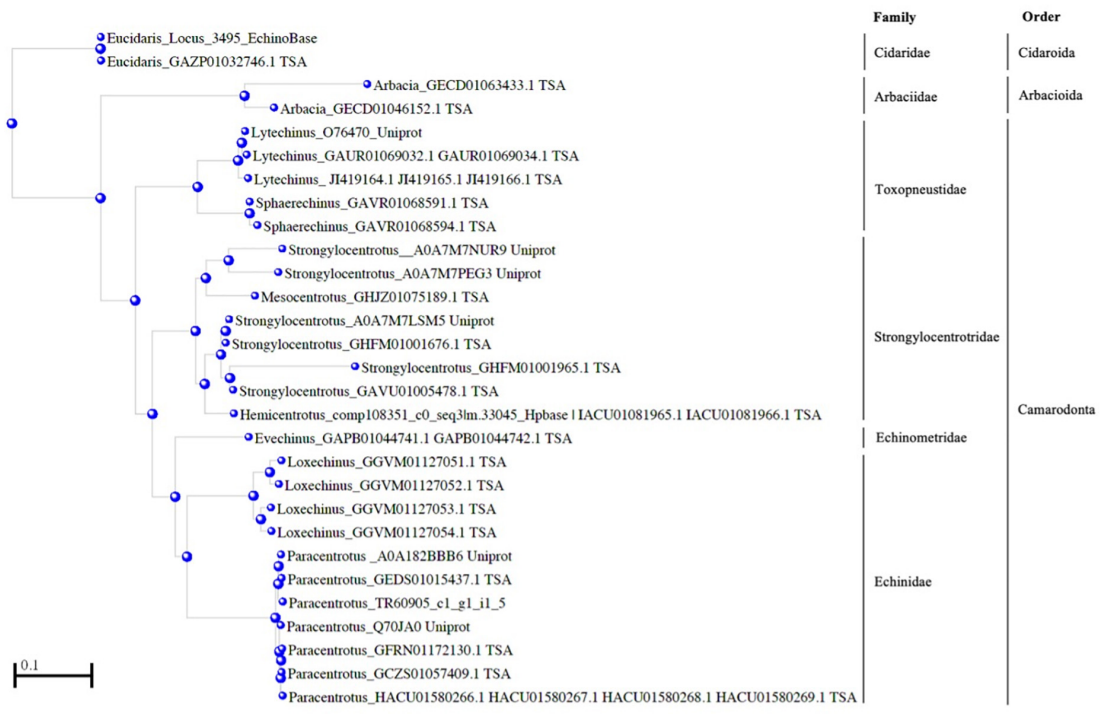

FIGURE 3 | Amino acid similarity between *Paracentrotus lividus* Nectin and homologous proteins from ten other sea urchin species. A tree from given distances between sequences was produced using the algorithm Fast Minimum Evolution (Desper and Gascuel, 2004) available at COBALT. The scale bar indicates an evolutionary distance of 0.2 aa substitutions per position in the sequence. Sea urchin phylogeny according to Koch and Thompson (2020) is presented next to the tree (see also **Figure 9**), indicated by the corresponding orders and families of the analyzed species: *Arbacia punctulata*, *Eucidaris tribuloides*, *Evechinus chloroticus*, *Hemicentrotus pulcherrimus*, *Loxechinus albus*, *Lytechinus variegatus*, *Mesocentrotus franciscanus*, *Sphaerechinus granularis* and *Strongylocentrotus purpuratus*. Sequences were retrieved at UniprotKB, Transcriptome Shotgun Assembly Sequence Database, EchinoBase, HpBase and Pjeta et al. (2020).

In *D. africanum*, the antibody only cross-reacted with an area containing pigment cells (**Figures 2E,I**). As for the labeling of the adhesive footprints, it was stronger in *P. lividus* and *S. granularis* than in *A. lixula* and *D. africanum* (**Figures 2M–P**), however, differences in total corrected fluorescence were only significant relatively to *D. africanum* (p-value$_{ANOVA}$ = 0.014) (**Figure 4** and **Supplementary Table 3**). In terms of protein labeling in western blots, many protein bands were detected by the anti-*P. lividus* Nectin antibody both in the disc and stem extracts in the four echinoids, but some high molecular weight bands (>100 kDa) were only present in the disc extracts in *A. lixula*, *P. lividus* and *S. granularis* (**Figure 5A**).

Glycans Associated With Adhesion-Related Proteins Vary Among Echinoid Species

Tube foot sections from the four echinoids from Madeira Island were stained with Alcian blue pH 2.5 to detect sulfated and carboxylated acidic mucopolysaccharides and sialomucins (i.e., mucins and glycoproteins with carboxyl group-containing sugars such as sialic, uronic and hyaluronic acids). The disc adhesive epidermis of *A. lixula* was strongly stained (**Figure 6B**), contrasting with moderate staining observed in *D. africanum* and *P. lividus* (**Figures 6A,C**), the weakest staining being exhibited by *S. granularis* (**Figure 6D**).

Through lectin histochemistry and lectin-blotting, we localized specific glycans in tube foot sections, footprints, and disc and stem extracts of these same species. GSL II which detects α- and β-linked N-acetylglucosamine residues (**Figures 7A–D**, **8A–D**, **Supplementary Table 1**) labeled strongly and specifically the cuticle covering the adhesive epidermis in *S. granularis* (**Figures 7D,Z**), and moderately labeled the adhesive epidermis of *P. lividus* (**Figures 7C,X**). In footprints, GSL II produced a significantly stronger labeling in *S. granularis* compared to the remaining three species (P_{ANOVA} = 0.0112) (**Figures 8A–D**, **9A** and **Supplementary Table 3**). This lectin labeled two glycoproteins around 75 and 135 kDa in both the disc and stem extracts from the four species, but in *S. granularis* a few additional disc-specific glycoproteins were strongly labeled at 35, 63 and > 100 kDa (**Figure 5B**). WGA, STL and LEL detect N-acetylglucosamine (GlcNac) in a specific chitobiose arrangement, i.e., a dimer of β-1,4-linked glucosamine units (**Figures 7E–P**, **8E–P Supplementary Table 3**). WGA, which detects up to two units GlcNacβ(1,4)GlcNac, produced results very similar to GSL II. It strongly labeled the adhesive epidermis of *P. lividus* (**Figures 7G,X**) and the cuticle covering the disc adhesive epidermis in *S. granularis* (**Figures 7H,Z**). Footprint labeling was also more intense in *S. granularis* (P_{ANOVA} = 0.0212) (**Figures 8E–H**, **9B** and **Supplementary Table 3**). In the lectin-blots, the same 75 and 135 kDa glycoproteins were detected in both the disc and stem extracts from the four species, but *S. granularis* disc-specific glycoproteins were more intensely labeled, together with a 35kDa band in *P. lividus* discs (**Figure 5C**). Between STL and LEL, which detect a higher number of GlcNacβ(1,4)GlcNac units (**Supplementary Table 1**), LEL was the one that produced the most relevant data (**Figures 7K–O,L–P**). It strongly labeled *P. lividus* disc epidermis (**Figures 7O,X**), its footprints (P_{ANOVA} = 0.0033) (**Figures 8M**, **9D** and **Supplementary Table 3**), and disc-specific glycoproteins at 35 and >135 kDa (**Figures 5D–E**). As for SBA, which detects terminal α- and β-linked N-acetylgalactosamine (**Figures 7Q–T**, **8Q–T**), it labeled the disc adhesive epidermis of *D. africanum* (**Figures 7Q,U**) and slightly labeled the disc-specific glycoproteins mentioned above for *S. granularis* and *P. lividus* (**Figure 5F**).

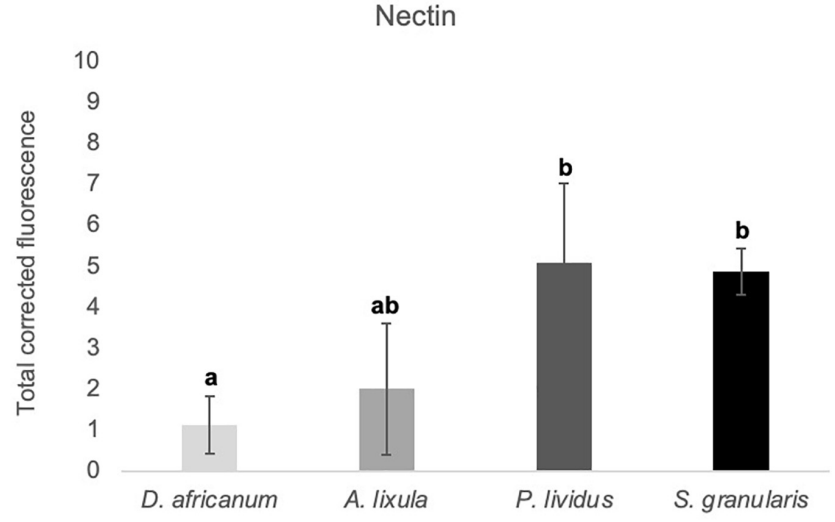

FIGURE 4 | Total corrected fluorescence (TCF) of footprints deposited by the adoral tube feet of *Diadema africanum*, *Arbacia lixula*, *Paracentrotus lividus*, and *Sphaerechinus granularis*, labeled with anti-*P. lividus* Nectin. TCF units are arbitrary. Data are expressed as means ± SD in each species. Significant interspecific differences between means for a given antibody are indicated by letters in superscript; means sharing at least one letter are not significantly different ($P > 0.05$, multiple comparison test of Tukey).

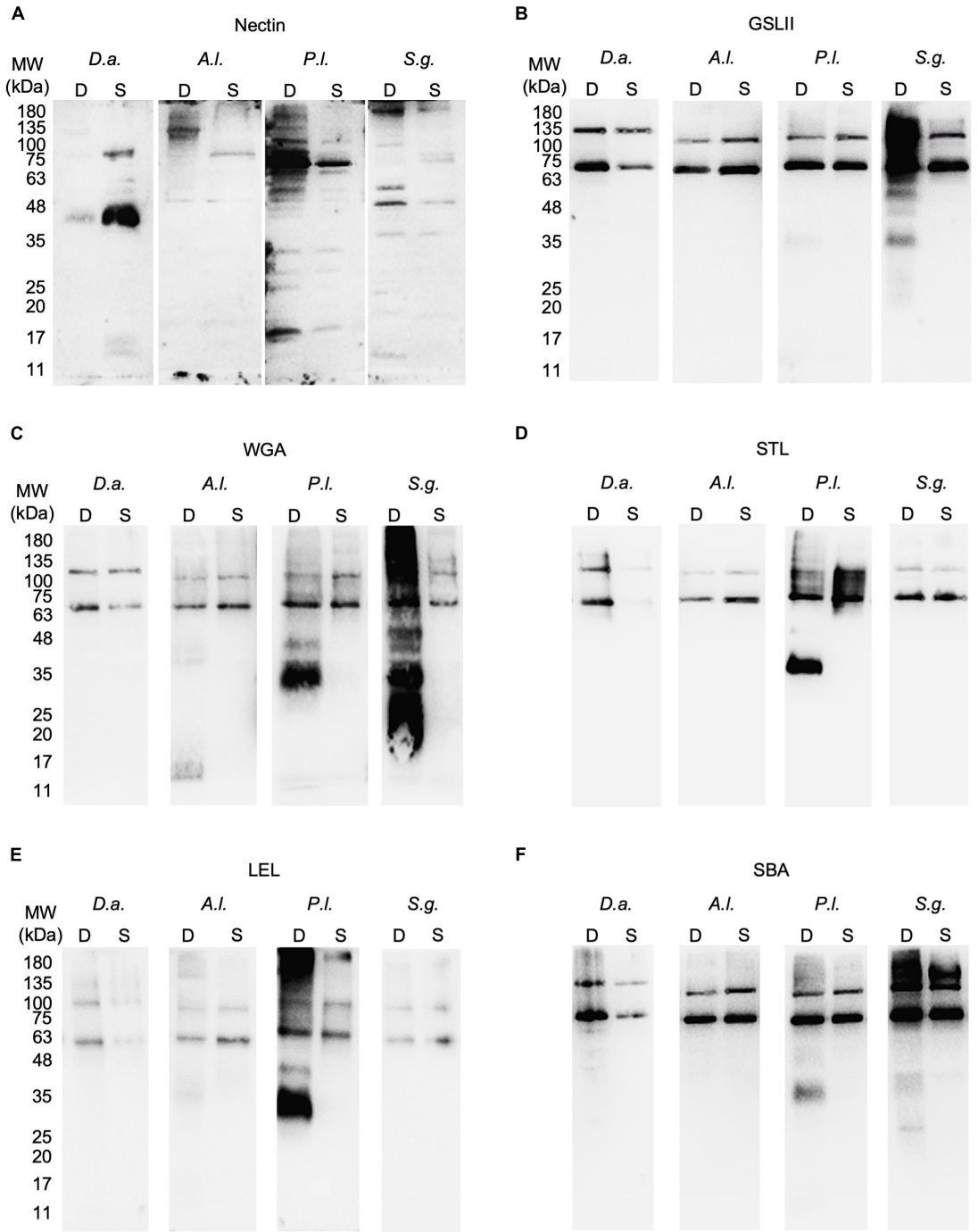

FIGURE 5 | Protein and glycoproteins detected in tube foot disc and stem extracts from *Diadema africanum*, *Arbacia lixula*, *Paracentrotus lividus* and *Sphaerechinus granularis* using *P. lividus* Nectin antibody **(A)** and five lectins **(B–F)** respectively, GSL II, WGA, STL, LEL, and SBA. GSL II was used to detect proteins conjugated with *N*-acetylglucosamine; WGA, STL and LEL to detect chitobiose and SBA to detect *N*-acetylgalactosamine. Al, *Arbacia lixula*; D, disc; Da, *Diadema africanum*; GSL II, *Griffonia simplicifolia* lectin II; LEL, *Lycopersicon esculentum* lectin; MW, molecular weight markers; Pl, *Paracentrotus lividus*; S, stem; SBA, Soybean agglutinin; Sg, *Sphaerechinus granularis*; STL, *Solanum tuberosum* lectin; WGA, wheat germ agglutinin.

DISCUSSION

Increasing interest in biological adhesives has been partly driven by the demand for novel biomimetic adhesives with capabilities beyond the synthetic glues currently available to consumers (Davey et al., 2021). However, the precise mechanisms responsible for the superiority of natural bioadhesives remain largely unknown. Adhesives secreted by aquatic invertebrates

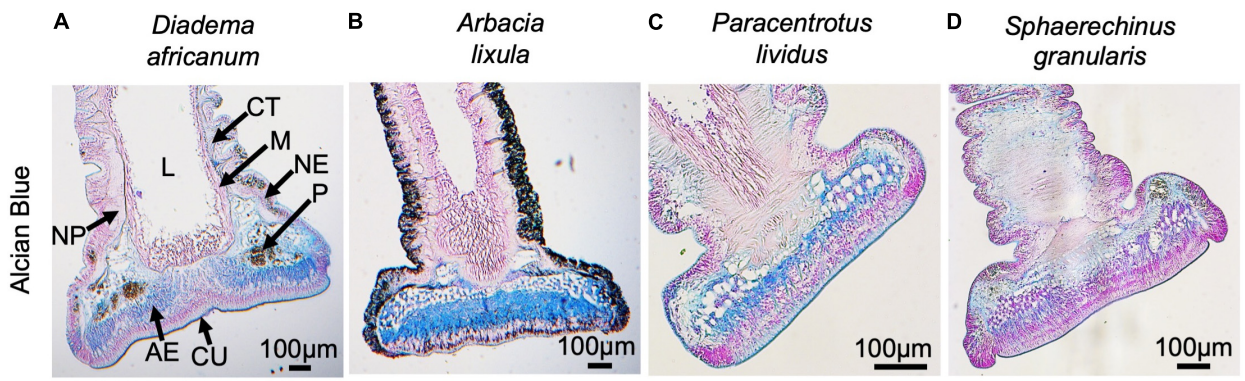

FIGURE 6 | Histological structure of adoral tube feet from *Diadema africanum* **(A)**, *Arbacia lixula* **(B)**, *Paracentrotus lividus* **(C)** and *Sphaerechinus granularis* **(D)** stained with Alcian Blue pH 2.5 (longitudinal sections). AE, adhesive epidermis; CT, connective tissue; CU, cuticle; L, lumen; M, myomesothelium; NE, non-adhesive epidermis; NP, nerve plexus, P, pigment cells.

contain proteins, glycans and lipids in varying proportions, as well as metals involved in crosslinking (Richter et al., 2018). Although adhesives from a growing number of organisms belonging to different taxa have been characterized, these studies are often based on a single species (Lengerer et al., 2019). More interspecific comparisons between closely related and unrelated species are needed to identify shared features, such as biased amino acid distribution, repetitive regions, and recurrent functional domains in putative adhesive and cohesive proteins. This information can provide clues on the key components of future biomimetic adhesives based on a particular amino acid (e.g., catechol-containing polymers inspired by DOPA in mussels; North et al., 2017), or on protein sequence repetitive regions and recurrent functional domains (e.g., functional domain-containing recombinant proteins based on the sequence of sea star Sfp1, Lefevre et al., 2020).

Recent comparative inter-phylum analyses of adhesive proteins revealed conserved blocks of different domains indicative of common evolutionary origin (Davey et al., 2021). It is currently known that the association of the domains vWD–C8–TIL, typical of vertebrate gel-forming secreted proteins like mucins, is recurrent in aquatic putative adhesive and cohesive protein such as sea urchin alpha-tectorin like protein (TR63383_c2_g1_i1), sea star Sfp1 (echinoderm), flatworm Mlig-ap1 and −2 (platyhelminth), and limpet P-vulgata_3 (mollusc) (Hennebert et al., 2014; Wunderer et al., 2019; Kang et al., 2020; Pjeta et al., 2020). This might indicate that these proteins evolved from a common mucin-like ancestor (Davey et al., 2021).

To find sequence conservation at the amino acid level, interspecific comparisons within the same phylum or lower taxonomic levels must be performed. In sea stars, Sfp1-like sequences were found in 17 species, representative of 10 families from four orders (Lengerer et al., 2019). However, high sequence variability between the species, prevented the use of an antibody directed against a specific peptide of Sfp1, thus restricting cross-immunoreactivity within the disc adhesive epidermis to two out of the 24 tested species (Lengerer et al., 2019). In sea urchins, no cross-reactivity was found in the adhesive disc epidermis of seven species belonging to three orders and five families of the Class Echinoidea using an antibody raised against the bulk adhesive of one species (Santos and Flammang, 2012).

In the present study, we demonstrated that an antibody against *P. lividus* Nectin whole protein produces cross-immunoreactivity in the tube foot epidermis and/or in the adhesive footprints of the four tested species belonging to four families (Diadematidae, Arbaciidae, Toxopneustidae, and Echinidae) and three orders (Diadematoida, Arbacioida, and Camarodonta) (**Figure 10**). More intense labeling, possibly indicative of a higher protein sequence homology and consequently higher antibody affinity, was observed in *S. granularis* which is phylogenetically closer to *P. lividus* (both belong to order Camarodonta). A similar result was obtained when we compared Nectin-like protein sequences from ten species belonging to six families (Cidaridae, Arbaciidae, Toxopneustidae, Strongylocentrotidae, Echinometridae, and Echinidae) and three orders (Cidaroida, Arbacioida, and Camarodonta). Closely related species belonging to the same family have Nectins with higher sequence homology (**Supplementary Table 2**).

Our immunohistochemical assays show that Nectin-like proteins are present both in the non-adhesive stem and in the adhesive disc of *P. lividus*, *D. africanum*, *A. lixula* and *S. granularis*, indicating that, in adult sea urchins, it might maintain an important cell adhesion role. However, a role in tube foot adhesion cannot be discarded because Nectin is consistently present in adhesive footprints. Moreover, like sea star Sfp1, it possesses several tandemly repeated discoidin-like (or F5/8 type C) domains, which allow protein-carbohydrate interactions. However, Sfp1 is more clearly associated with sea star tube foot adhesion because it is present exclusively in the adhesive granules of all the species studied (Hennebert et al., 2014; Lengerer et al., 2019).

The use of five lectins to detect N-acetylglucosamine (GSL II), chitobiose (WGA, STL, LEL) and N-acetylgalactosamine (SBA), confirmed that LEL produces a strong specific labeling of *P. lividus* tube foot adhesive epidermis and footprints indicating that the adhesive in this species contains *N*-acetyl-D-glucosamine

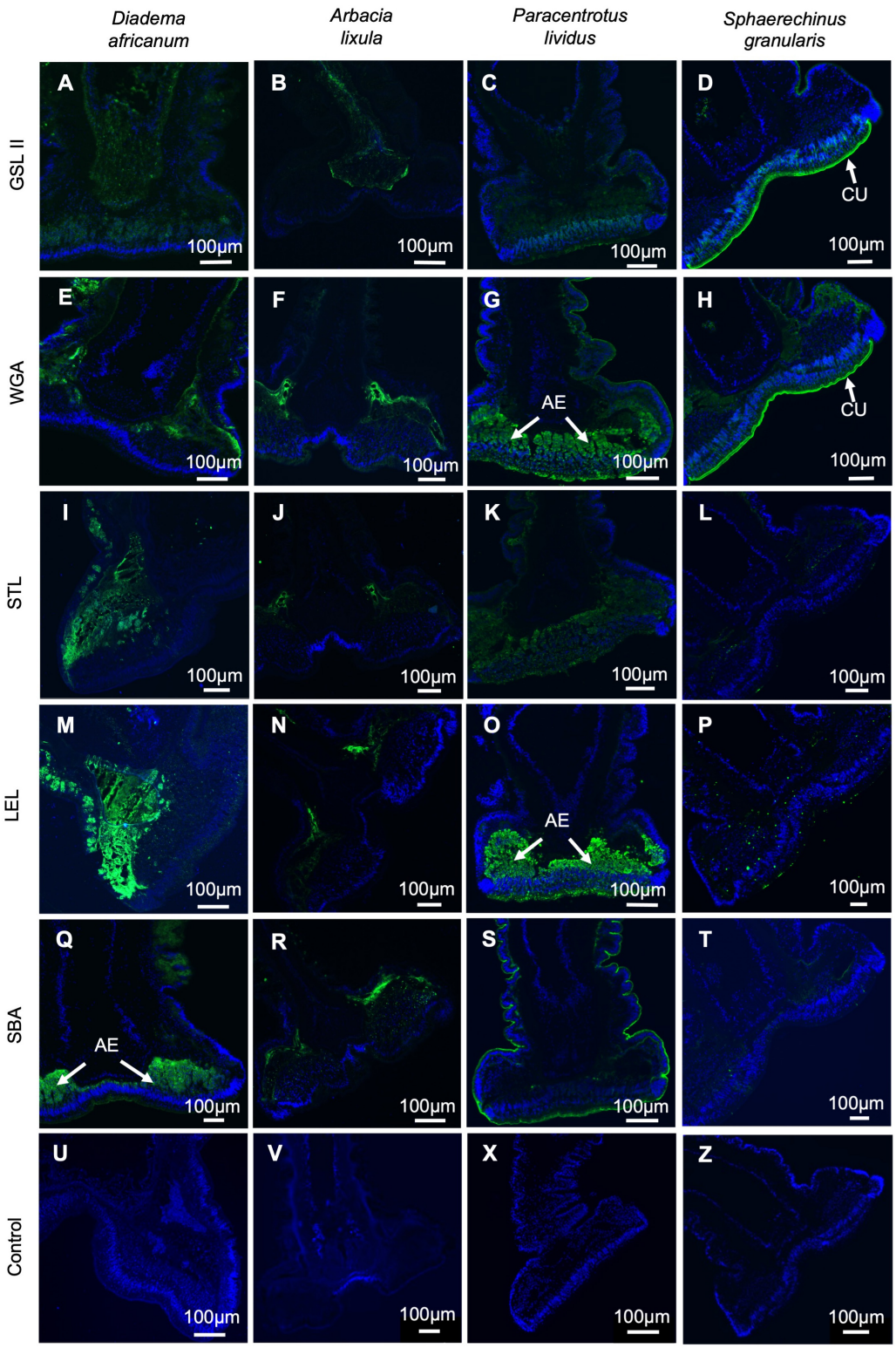

FIGURE 7 | Lectin histochemistry on longitudinal sections through adoral tube feet from *Diadema africanum* **(A,E,I,M,Q,U)**, *Arbacia lixula* **(B,F,J,N,R,V)**, *Paracentrotus lividus* **(C,G,K,O,S,W)** and *Sphaerechinus granularis* **(D,H,L,P,T,X)**. Labeling (in green) of *N*-acetylglucosamine using GSL II **(E–H)**; chitobiose using WGA **(I–L)**, STL **(M-P)** and LEL **(Q–T)**, and *N*-acetylgalactosamine using SBA **(U–X)**. Negative controls **(U–Z)** in which the lectin has been replaced by buffer. AE, adhesive epidermis; CU, cuticle; GSL II, *Griffonia simplicifolia* lectin II; LEL, *Lycopersicon esculentum* lectin; SBA, Soybean agglutinin; STL, *Solanum tuberosum* lectin; WGA, wheat germ agglutinin.

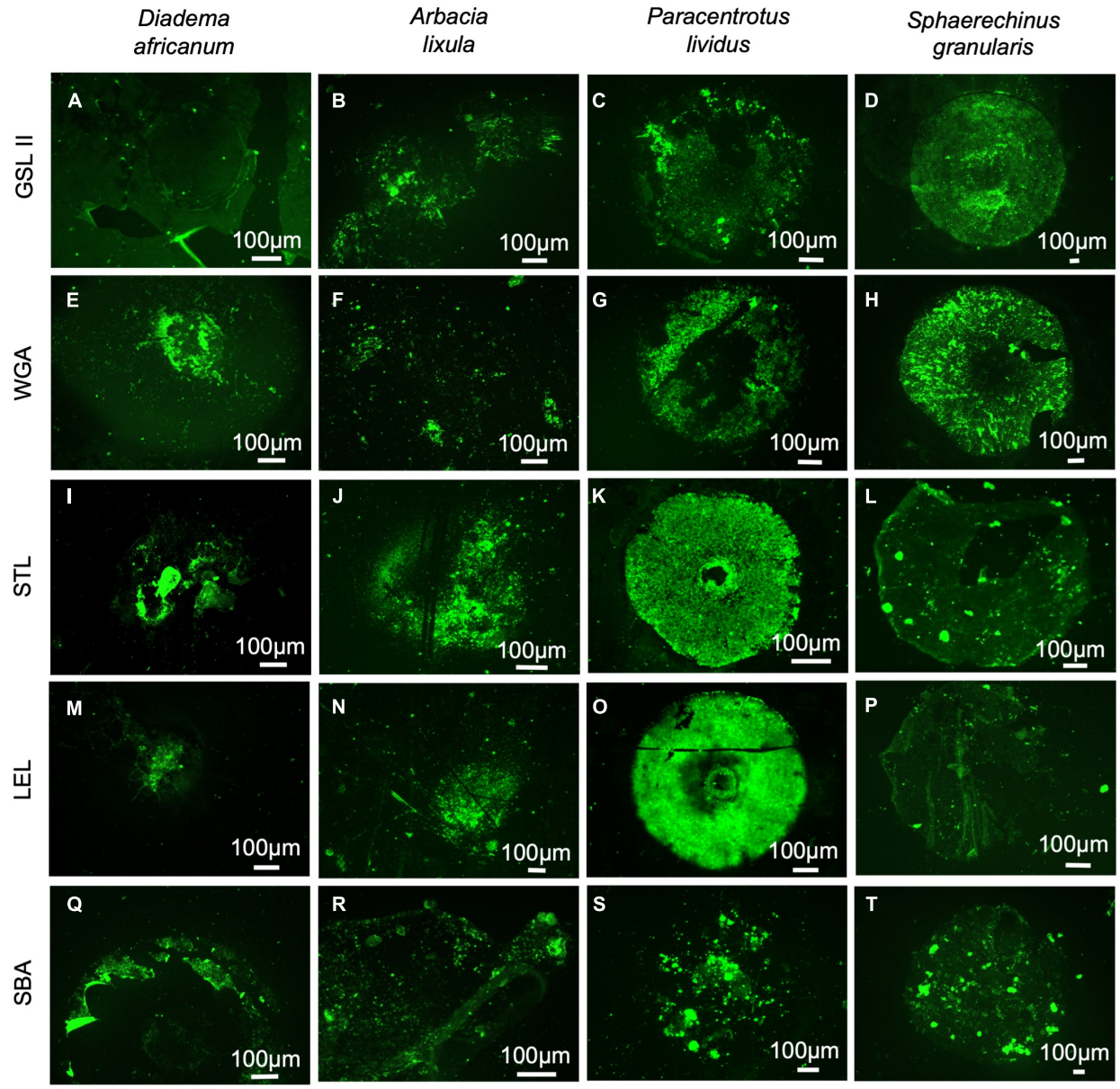

FIGURE 8 | Lectin histochemistry of footprints deposited by adoral tube feet from *Diadema africanum* **(A,E,I,M,Q)**, *Arbacia lixula* **(B,F,J,N,R)**, *Paracentrotus lividus* **(C,G,K,O,S)** and *Sphaerechinus granularis* **(D,H,L,P,T)** using GSL II to detect *N*-acetylglucosamine **(A–D)**; WGA **(E–H)**, STL **(I–L)** and LEL **(M–P)** to detect chitobiose; and SBA **(Q–T)** do detect *N*-acetylgalactosamine. GSL II, *Griffonia simplicifolia* lectin II; LEL, *Lycopersicon esculentum* lectin; SBA, Soybean agglutinin; STL, *Solanum tuberosum* lectin; WGA, wheat germ agglutinin.

β (1,4)N-acetyl-D-glucosamine oligomers with up to 4 carbohydrate units (Simão et al., 2020). Interestingly, in *S. granularis*, also from the order Camarodonta, it was WGA (and GSL II to a minor extent) which produced an intense labeling of the footprints and the cuticle covering the adhesive epidermis. This indicates that the adhesive in *S. granularis* also contains chitobiose but with a lower number of units than in *P. lividus*. These glycans seem to be conjugated to proteins since LEL in *P. lividus* and WGA in *S. granularis* pinpointed strongly labeled bands at 35 and > 100kDa (**Figure 10**). Whether these glycoproteins are homologous remains unanswered, but similar glycans in phylogenetically related species are demonstrated here. For *A. lixula*, no specific labeling was obtained with the tested lectins. The tube foot adhesive epidermis in *D. africanum* was stained with SBA, suggesting the presence of N-acetylgalactosamine, but lectin-blots did not corroborate this. The lectin-blots also revealed the presence of two glycoproteins (around 75 and 135 kDa) containing N-acetylglucosamine and N-acetylgalactosamine residues that are conserved in all the species, being present both in disc and

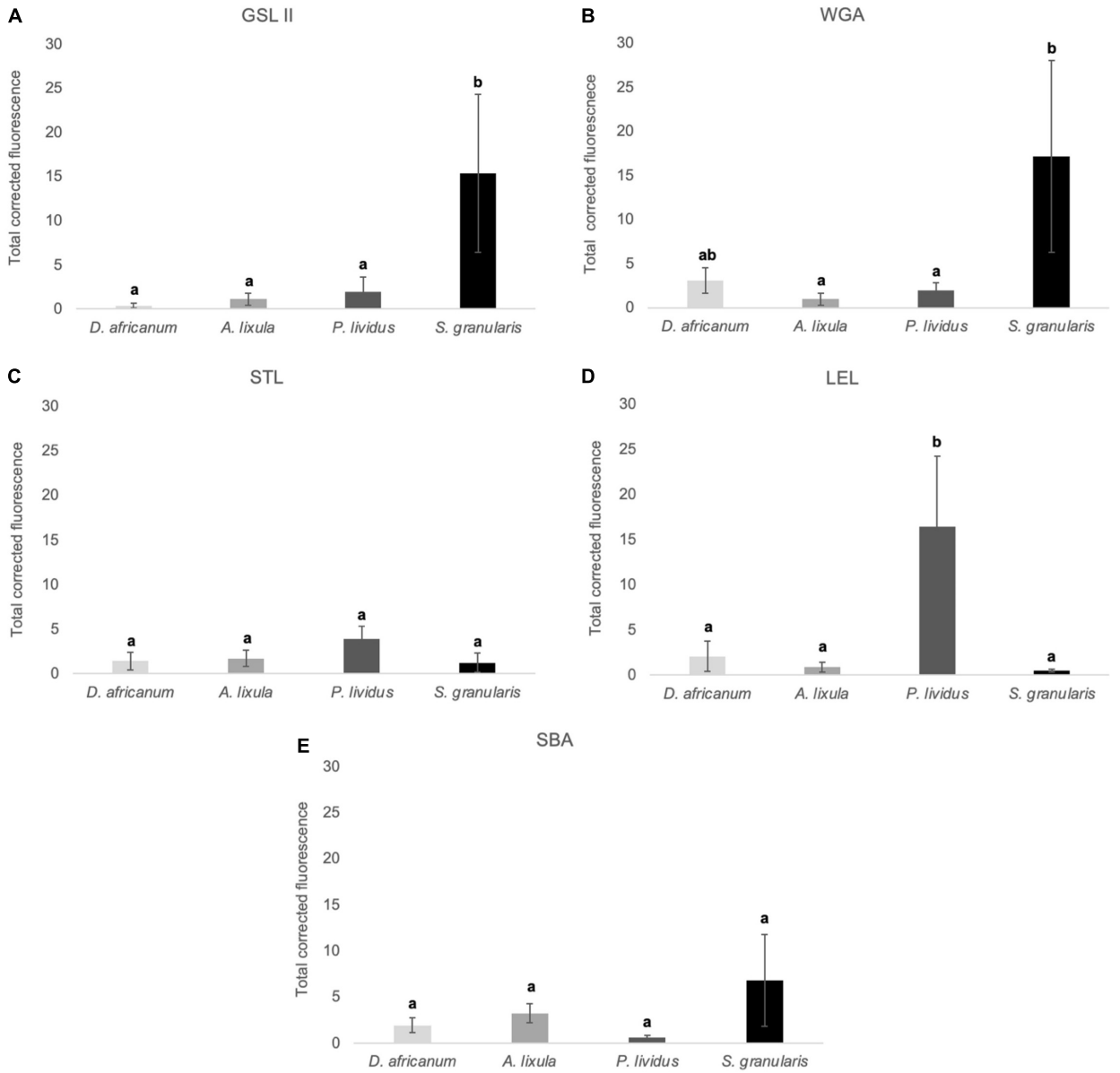

FIGURE 9 | Total corrected fluorescence (TCF) of footprints deposited by the adoral tube feet of *Diadema africanum*, *Arbacia lixula*, *Paracentrotus lividus* and *Sphaerechinus granularis*, and labelled with GSLII **(A)**, WGA **(B)**, STL **(C)**, LEL **(D)** and SBA **(E)**. TCF units are arbitrary. Data are expressed as means ± SD in each species. Significant interspecific differences between means for a given lectin are indicated by letters in superscript; means sharing at least one letter are not significantly different ($P > 0.05$, multiple comparison test of Tukey).

stem extracts. These two proteins had been previously reported in *P. lividus*, being present in the cytoplasm and microvilli of epidermal support cells (Simão et al., 2020). Torn microvilli might explain the fluorescent labeling observed in the footprints of all the species with the five tested lectins.

Future studies should perform a full lectin screening for each sea urchin since the composition of the glycosidic fraction of their adhesives seems to be quite variable between species. It should also be stressed that lectins produced much higher corrected fluorescence of the footprints (**Figures 4**, **9**) and a more precise detection of disc-specific proteins (**Figure 5**) than antibodies. One explanation could be that Nectin detected by the antibody used, is not so relevant for sea urchin adhesion, compared to other glycoproteins detected by the lectins. Glycoproteins are ubiquitous in aquatic adhesives (see Introduction) and glycosylation is pointed to increase conformational stability, enhance protein-binding ability, and make proteins more resistant to degradation (Rzepecki and Waite, 1993; Smith et al., 1999; Smith and Morin, 2002; Ohkawa et al., 2004; Urushida et al., 2007; Zhao et al., 2009; Hennebert et al., 2011, 2014; Pagett et al., 2012; Roth et al., 2012; Wunderer et al., 2019).

Our study demonstrates that although the external morphology of sea urchin tube feet is quite alike, their histology and secretory granule ultrastructure vary between species.

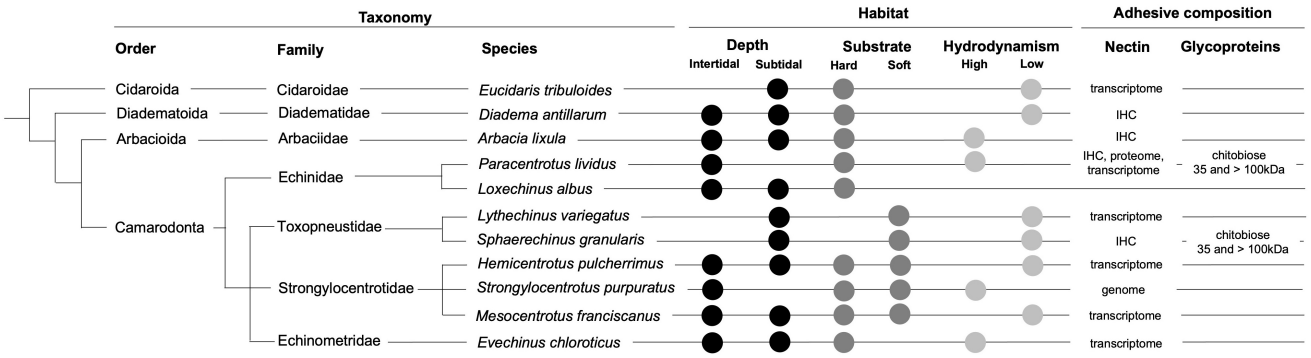

FIGURE 10 | Taxonomy, habitat, and adhesive composition of the analyzed echinoid species. Phylogeny according to Koch and Thompson (2020). Habitat information provided by https://www.sealifebase.ca and http://www.marinespecies.org/echinoidea/. IHC, immunohistochemistry.

As hypothesized by Santos and Flammang (2006), species inhabiting hard substrata in areas with high hydrodynamic forces possess more robust tube foot discs (with denser skeletal elements and thicker muscle and connective tissue layers) than species typical of soft substrata in less exposed habitats. Disc morphology appears independent of tube foot tenacity, since the adhesive force per unit area of individual sea urchins from species with contrasted morphology, taxonomy and ecology is not markedly different (Santos and Flammang, 2006, 2008). What seems to be a significant selective pressure to determine habitat distribution, is the size and shape of the sea urchins. *D. africanum* with its long thin spines and *S. granularis* with its big, rounded test are morphologically less adapted to cope with hydrodynamism, being dislodged at lower water velocities than *A. lixula* and *P. lividus* (Santos and Flammang, 2007; Tuya et al., 2007). Thus, interspecific tenacity differences seem to be related to dissimilarities in the adhesive composition. A considerable variation in the internal organization of adhesive secretory granules has been observed, but no correlation could be established with taxonomy, habitat, or tube foot morphology (Santos and Flammang, 2006; present study). Although we analyzed tube feet from at least three animals with different test size per species, no influence of age on secretory granule ultrastructure was found either. However, accurate estimation of sea urchin age is still a subject that remains open to discussion (Russell and Meredith, 2000; Narvaez et al., 2016). The present study revealed conservation of Nectin-like proteins among the eleven studied species, but a significant variation of the glycan residues that compose their footprints. However, taxonomically closer species, like *P. lividus* and *S. granularis*, seem to possess putative adhesive glycoproteins with similar molecular weights (35 and > 100kDa) and glycans (chitobiose - disaccharides of β-1,4-linked glucosamine units) although with a different number of repetitive oligomers. Nectin, via its discoidin domains, can bind the N-acetylglucosamine carbohydrate moieties (Costa et al., 2010) present in the adhesive glycoproteins, contributing to connect the disc epidermis to the adhesive secretion and thus increasing the cohesion of this interface. The adhesive footprint interspecific glycan variability might also have implications for the enzymatic de-adhesion of temporary attaching marine animals (Lengerer and Ladurner, 2018). Indeed, proteases and glycosidases have been detected in the footprint proteome of the sea star *A. rubens* (Hennebert et al., 2015), and are also highly over-expressed in sea urchin *P. lividus* adhesive discs relatively to non-adhesive stems (Lebesgue et al., 2016). Provided that a de-adhesive enzyme-based secretion would cleave the bond between the tube foot cuticle and the adhesive material (Lengerer and Ladurner, 2018), it should be specific to the protein and glycan composition of each species. This hypothesis should be investigated in future studies.

Finally, our findings support data reported on sea stars and barnacles showing that in large structural proteins (like Sfp1 in sea stars, cp-100 k in barnacles and Nectin in sea urchin), the selection pressure is high for the conservation of functional domains (He et al., 2018; Lengerer et al., 2019). The same authors suggested that in small surface-binding proteins, the relative amino acid composition is more variable, being potentially more influenced by adaptations to the habitat and mode of living. More genomic data and tube foot-specific transcriptomes would be required for sea urchins to allow further comparisons of full-length protein sequences. This study shows that post-translational modifications like glycosylation must be taken in the equation since we found evidence of large variation in terms of the conjugated glycans, but with indications of taxonomy-related conservation.

DATA AVAILABILITY STATEMENT

The datasets presented in this study can be found in online repositories. The names of the repository/repositories and accession number(s) can be found in the article/ **Supplementary Material**.

AUTHOR CONTRIBUTIONS

RJ and RL collected the specimens. LG, PF, PR, and NN performed the experiments. LG and RS performed data and statistical analysis. RS, NN, JM, and JC-C contributed to the conception and design of the study. RS and PF wrote the first

draft of the manuscript. All authors contributed to manuscript revision, read, and approved the submitted version.

FUNDING

This publication was financed by Portuguese National Funds through FCT – Fundação IP strategic project UIDB/04292/2020 awarded to MARE, and by the European Union's Horizon 2020 Research and Innovation Programme under grant agreement N810139: Project Portugal Twinning for Innovation and Excellence in Marine Science and Earth Observation – PORTWIMS. PR was financially supported by the Oceanic Observatory of Madeira Project (M1420-01-0145-FEDER-000001-Observatório Oceânico da Madeira-OOM), co-financed by the Madeira Regional Operational Programme (Madeira 14–20), under the Portugal 2020 strategy, through the European Regional Development Fund (ERDF). PF was supported by the Fund for Scientific Research of Belgium (F.R.S.-FNRS) "Projet de Recherche" T.0088.20. JM was supported by a post-doctoral research fellowship by Agência Regional para o Desenvolvimento da Investigação, Tecnologia e Inovação (ARDITI–M1420-09-5369-FSE-000002). JC-C and RS are funded by national funds through FCT under the Scientific Employment Stimulus - Institutional Call - [CEECINST/00098/2018, CEECINST/00032/2018/CP1523/CT006].

ACKNOWLEDGMENTS

The authors would like to thank FCUL Microscopy Facility for providing access to fluorescence microscope. Faculty of Sciences of the University of Lisbon's Microscopy Facility is a node of the Portuguese Platform of BioImaging, reference PPBI-POCI-01-0145-FEDER-022122. The authors also acknowledge Francesca Zito (Istituto per la Ricerca e l'Innovazione Biomedica, Consiglio Nazionale delle Ricerche, Italy) for providing antibodies. PF is Research Director of the F.R.S.- FNRS.

SUPPLEMENTARY MATERIAL

The Supplementary Material for this article can be found online at: https://www.frontiersin.org/articles/10.3389/fmars.2021.737886/full#supplementary-material

REFERENCES

Costa, C., Cavalcante, C., Zito, F., Yokota, Y., and Matranga, V. (2010). Phylogenetic analysis and homology modelling of *Paracentrotus lividus* Nectin. *Mol. Divers.* 14, 653–665. doi: 10.1007/s11030-009-9203-3

Davey, P. A., Power, A. M., Santos, R., Bertemes, P., Ladurner, P., Palmowski, P., et al. (2021). Omics-based molecular analyses of adhesion by aquatic invertebrates. *Biol. Rev.* 96, 1051–1075. doi: 10.1111/brv.12691

Desper, R., and Gascuel, O. (2004). Theoretical foundation of the balanced minimum evolution method of phylogenetic inference and its relationship to weighted least-squares tree fitting. *Mol. Biol. Evol.* 21, 587–598. doi: 10.1093/molbev/msh049

Dreanno, C., Matsumura, K., Dohmae, N., Takio, K., Hirota, H., Kirby, R. R., et al. (2006). An alpha(2)-macroglobulin like protein is the cue to gregarious settlement of the barnacle *Balanus amphitrite*. *Proc. Natl. Acad. Sci. U. S. A.* 103, 14396–14401. doi: 10.1073/pnas.0602763103

Ferrier, G. A., Kim, S. J., Kaddis, C. S., Loo, J. A., Zimmer, C. A., and Zimmer, R. K. (2016). Multifuncin: a multifunctional protein cue induces habitat selection by, and predation on, barnacles. *Integr. Comp. Biol.* 56, 901–913. doi: 10.1093/icb/icw076

He, L. S., Zhang, G., Wang, Y., Yan, G. Y., and Qian, P. Y. (2018). Toward understanding barnacle cementing by characterization of one cement protein-100 kDa in *Amphibalanus amphitrite*. *Biochem. Biophys. Res. Commun.* 495, 969–975. doi: 10.1016/j.bbrc.2017.11.101

Hennebert, E., Leroy, B., Wattiez, R., and Ladurner, P. (2015). An integrated transcriptomic and proteomic analysis of sea star epidermal secretions identifies proteins involved in defense and adhesion. *J. Proteomics* 128, 83–91. doi: 10.1016/j.jprot.2015.07.002

Hennebert, E., Wattiez, R., Demeuldre, M., Ladurner, P., Hwang, D. S., Waite, J. H., et al. (2014). Sea star tenacity mediated by a protein that fragments, then aggregates. *Proc. Natl. Acad. Sci. U. S. A.* 111, 6317–6322. doi: 10.1073/pnas.1400089111

Hennebert, E., Wattiez, R., and Flammang, P. (2011). Characterisation of the carbohydrate fraction of the temporary adhesive secreted by the tube feet of the sea star *Asterias rubens*. *Mar. Biotechnol.* 13, 484–495. doi: 10.1007/s10126-010-9319-6

Kang, V., Lengerer, B., Wattiez, R., and Flammang, P. (2020). Molecular insights into the powerful mucus-based adhesion of limpets (*Patella vulgata* L.). *Open Biol.* 10:200019. doi: 10.1098/rsob.200019

Koch, N. M., and Thompson, J. R. (2020). A Total-evidence dated phylogeny of echinoids and the evolution of body size across adaptive landscape. *bioRxiv* [Preprint]. doi: 10.1101/2020.02.13.947796

Lebesgue, N., da Costa, G., Ribeiro, R. M., Ribeiro-Silva, C., Martins, G. G., Matranga, V., et al. (2016). Deciphering the molecular mechanisms underlying sea urchin reversible adhesion: a quantitative proteomics approach. *J. Proteomics* 138, 61–71. doi: 10.1016/j.jprot.2016.02.026

Lefevre, M., Flammang, P., Aranko, A. S., Linder, M. B., Scheibel, T. R., Humenik, M., et al. (2020). Sea star-inspired recombinant adhesive proteins self-assemble and adsorb on surfaces in aqueous environments to form cytocompatible coatings. *Acta Biomater.* 112, 62–74. doi: 10.1016/j.actbio.2020.05.036

Lengerer, B., Algrain, M., Lefevre, M., Delroisse, J., Hennebert, E., and Flammang, P. (2019). Interspecies comparison of sea star adhesive proteins. *Philos. Trans. R. Soc. Lond. B Biol. Sci.* 374:20190195. doi: 10.1098/rstb.2019.0195

Lengerer, B., and Ladurner, P. (2018). Properties of temporary adhesion systems of marine and freshwater organisms. *J. Exp. Biol.* 221:jeb182717. doi: 10.1242/jeb.182717

Li, S., Huang, X., Chen, Y., Li, X., and Zhan, A. (2019). Identification and characterization of proteins involved in stolon adhesion in the highly invasive fouling ascidian *Ciona robusta*. *Biochem. Biophys. Res. Commun.* 510, 91–96. doi: 10.1016/j.bbrc.2019.01.053

Narvaez, C. A., Johnson, L. E., and Sainte-Marie, B. (2016). Growth bands are an unreliable indicator of sea urchin age: evidence from the laboratory and the literature. *Limnol. Oceanogr. Methods* 14, 527–541.

North, M. A., Del Grosso, C. A., and Wilker, J. J. (2017). High strength underwater bonding with polymer mimics of mussel adhesive proteins. *ACS Appl. Mater. Interfaces* 9, 7866–7872. doi: 10.1021/acsami.7b00270

Ohkawa, K., Nishida, A., Yamamoto, H., and Waite, J. H. (2004). A Glycosylated byssal precursor protein from the green mussel *Perna viridis* with modified dopa side-chains. *Biofouling* 20, 101–115. doi: 10.1080/08927010410001681246

Pagett, H. E., Abrahams, J. L., Bones, J., O'Donoghue, N., Marles-Wright, J., Lewis, R. J., et al. (2012). Structural characterisation of the N-glycan moiety of the barnacle settlement-inducing protein complex (SIPC). *J. Exp. Biol.* 215(Pt 7), 1192–1198. doi: 10.1242/jeb.063503

Pjeta, R., Lindner, H., Kremser, L., Salvenmoser, W., Sobral, D., Ladurner, P., et al. (2020). Integrative transcriptome and proteome analysis of the tube foot and adhesive secretions of the sea urchin *Paracentrotus lividus*. *Int. J. Mol. Sci.* 21:946. doi: 10.3390/ijms21030946

Pjeta, R., Wunderer, J., Bertemes, P., Hofer, T., Salvenmoser, W., Lengerer, B., et al. (2019). Temporary adhesion of the proseriate flatworm *Minona ileanae*. *Philos. Trans. R. Soc. Lond. B Biol. Sci.* 374:20190194. doi: 10.1098/rstb.2019.0194

Richter, K., Grunwald, I., and Von Byern, J. (2018). "Bioadhesives," in *Handbook of Adhesion Technology*, eds L. da Silva, A. Oechsner, and R. Adams (Cham: Springer), 1–45.

Rodrigues, M., Ostermann, T., Kremeser, L., Lindner, H., Beisel, C., Berezikov, E., et al. (2016). Profiling of adhesive-related genes in the freshwater cnidarian *Hydra magnipapillata* by transcriptomics and proteomics. *Biofouling* 32, 1115–1129. doi: 10.1080/08927014.2016.1233325

Roth, Z., Yehezkel, G., and Khalaila, I. (2012). Identification and quantification of protein glycosylation. *Int. J. Carbohydr. Chem.* 2012:640923.

Rzepecki, L. M., and Waite, J. H. (1993). The byssus of the zebra mussel, *Dreissena polymorpha*. II: structure and polymorphism of byssal polyphenolic protein families. *Mol. Mar. Biol. Biotechnol.* 2, 267–279.

Russell, M. P., and Meredith, R. W. (2000). Natural growth lines in echinoid ossicles are not reliable indicators of age: a test using *Strongylocentrotus droebachiensis*. *Invertebr. Biol.* 119, 410–420.

Santos, R., Barreto, A., Franco, C., and Coelho, A. V. (2013). Mapping sea urchins tube feet proteome–a unique hydraulic mechano-sensory adhesive organ. *J. Proteomics* 79, 100–113. doi: 10.1016/j.jprot.2012.12.004

Santos, R., and Flammang, P. (2005). Morphometry and mechanical design of tube foot stems in sea urchins: a comparative study. *J. Exp. Mar. Biol. Ecol.* 315, 211–223. doi: 10.1016/j.jembe.2004.09.016

Santos, R., and Flammang, P. (2006). Morphology and tenacity of the tube foot disc of three common European sea urchin species: a comparative study. *Biofouling* 22, 187–200. doi: 10.1080/08927010600780771

Santos, R., and Flammang, P. (2007). Intra- and interspecific variation of attachment strength in sea urchins. *Mar. Ecol. Prog. Ser.* 332, 129–142.

Santos, R., and Flammang, P. (2008). Estimation of the attachment strength of the shingle sea urchin, *Colobocentrotus atratus*, and comparison with three sympatric echinoids. *Mar. Biol.* 154, 37–49. doi: 10.1007/s00227-007-0895-6

Santos, R., and Flammang, P. (2012). Is the adhesive material secreted by sea urchin tube feet species-specific?. *J. Morphol.* 273, 40–48. doi: 10.1002/jmor.11004

Santos, R., Haesaerts, D., Jangoux, M., and Flammang, P. (2005). Comparative histological and immunohistochemical study of sea star tube feet (Echinodermata, Asteroidea). *J. Morphol.* 263, 259–269. doi: 10.1002/jmor.10187

Santos, R., da Costa, G., Franco, C., Gomes-Alves, P., Flammang, P., and Coelho, A. V. (2009). First insights into the biochemistry of tube foot adhesive from the sea urchin *Paracentrotus lividus* (Echinoidea, Echinodermata). *Mar. Biotechnol.* 11, 686–698. doi: 10.1007/s10126-009-9182-5

Simão, M., Moço, M., Marques, L., and Santos, R. (2020). Characterization of the glycans involved in sea urchin *Paracentrotus lividus* reversible adhesion. *Mar. Biol.* 167:125.

Smith, A. B. (1978). A functional classification of the coronal pores of echinoids. *Palaeontology* 21, 759–789.

Smith, A. M., and Morin, M. C. (2002). Biochemical differences between trail mucus and adhesive mucus from marsh periwinkle snails. *Biol. Bull.* 203, 338–346. doi: 10.2307/1543576

Smith, A. M., Papaleo, C., Reid, C. W., and Bliss, J. M. (2017). RNA-Seq reveals a central role for lectin, C1q and von Willebrand factor A domains in the defensive glue of a terrestrial slug. *Biofouling* 33, 741–754. doi: 10.1080/08927014.2017.1361413

Smith, A. M., Quick, T. J., and St Peter, R. L. (1999). Differences in the composition of adhesive and non-adhesive mucus from the limpet *Lottia limatula*. *Biol. Bull.* 196, 34–44. doi: 10.2307/1543164

So, C. R., Scancella, J. M., Fears, K. P., Essock-Burns, T., Haynes, S. E., Leary, D. H., et al. (2017). Oxidase activity of the barnacle adhesive interface involves peroxide-dependent catechol oxidase and lysyl oxidase enzymes. *ACS Appl. Mater. Interfaces* 9, 11493–11505. doi: 10.1021/acsami.7b01185

Toubarro, D., Gouveia, A., Ribeiro, R. M., Simões, N., da Costa, G., Cordeiro, C., et al. (2016). Cloning, characterization, and expression levels of the Nectin gene from the tube feet of the sea urchin *Paracentrotus lividus*. *Mar. Biotechnol.* 18, 372–383. doi: 10.1007/s10126-016-9698-4

Tuya, F., Cisneros-Aguirre, J., Ortega-Borges, L., and Haroun, R. J. (2007). Bathymetric segregation of sea urchin on reefs of the Canarian Archipelago: role of flow-induced forces. *Estuar. Coast. Shelf Sci.* 73, 481–488.

Urushida, Y., Nakano, M., Matsuda, S., Inoue, N., Kanai, S., Kitamura, N., et al. (2007). Identification and functional characterization of a novel barnacle cement protein. *FEBS J.* 274, 4336–4346. doi: 10.1111/j.1742-4658.2007.05965.x

Viana, A. S., and Santos, R. (2018). Nanoscale characterization of the temporary adhesive of the sea urchin *Paracentrotus lividus*. *Beilstein J. Nanotechnol.* 9, 2277–2286. doi: 10.3762/bjnano.9.212

Wang, C.-S., Ashton, N. N., Weiss, R. B., and Stewart, R. J. (2014). PeroxiNectin catalyzed dityrosine crosslinking in the adhesive underwater silk of a casemaker caddisfly larvae, *Hysperophylax occidentalis*. *Insect Biochem. Mol. Biol.* 54, 69–79. doi: 10.1016/j.ibmb.2014.08.009

Wunderer, J., Lengerer, B., Pjeta, R., Bertemes, P., Kremser, L., Lindner, H., et al. (2019). A mechanism for temporary bioadhesion. *Proc. Natl. Acad. Sci. U. S. A.* 116, 4297–4306. doi: 10.1073/pnas.1814230116

Zeng, F., Wunderer, J., Salvenmoser, W., Ederth, T., and Rothbächer, U. (2019). Identifying adhesive components in a model tunicate. *Philos. Trans. R. Soc. Lond. B Biol. Sci.* 374:20190197. doi: 10.1098/rstb.2019.0197

Zhao, H., Sagert, J., Hwang, D. S., and Waite, J. H. (2009). Glycosylated hydroxytryptophan in a mussel adhesive protein from *Perna viridis*. *J. Biol. Chem.* 284, 23344–23352. doi: 10.1074/jbc.M109.022517

Zito, F., Burke, R. D., and Matranga, V. (2010). Pl-Nectin, a discoidin family member, is a ligand for betaC integrins in the sea urchin embryo. *Matrix Biol.* 29, 341–345. doi: 10.1016/j.matbio.2010.02.005

Zito, F., Nakano, E., Sciarrino, S., and Matranga, V. (2000). Regulative specification of ectoderm in skeleton disrupted sea urchin embryos treated with monoclonal antibody to Pl-nectin. *Dev. Growth Differ.* 42, 499–506. doi: 10.1046/j.1440-169x.2000.00531.x

Zito, F., Tesoro, V., McClay, D. R., Nakano, E., and Matranga, V. (1998). Ectoderm cell–ECM interaction is essential for sea urchin embryo skeletogenesis. *Dev. Biol.* 196, 184–192. doi: 10.1006/dbio.1998.8866

Conflict of Interest: The authors declare that the research was conducted in the absence of any commercial or financial relationships that could be construed as a potential conflict of interest.